Three-Dimensional Stress Fields in Finite Thickness Plate with Hole Under Shear Load

Dai Longchao(戴隆超)[1*], *Wang Xinwei*(王鑫伟)[2], *Gong Junjie*(龚俊杰)[1], *Gu Xiang*(顾乡)[1]

1. College of Mechanical Engineering, Yangzhou University, Yangzhou, 225127, P. R. China;
2. State Key Laboratory of Mechanics and Control of Mechanical Structures, Nanjing University of Aeronautics and Astronautics, Nanjing, 210016, P. R. China

(Received 19 April 2013; revised 5 September 2013; accepted 10 September 2013)

Abstract: The theoretical solutions are obtained for the three-dimensional (3-D) stress field in an infinite isotropic elastic plate with a through-the-thickness circular hole subjected to shear load at far field by using Kane and Mindlin's assumption based on the stress function method. Based on the present solutions, the characteristics of 3-D stress field are analyzed and the emphasis is placed on the effects of the plate thickness and Poisson's ratio on the deviation of the present 3-D in-plane stress from the related plane stress solutions, the stress concentration and the out-of-plane constraint. The present solutions show that the stress concentration factor reaches its peak value of about 8.9% which is higher than that of the plane stress solutions. As expected, the out-of-plane stress constraint factor can reach 1 on the surface of the hole when the plate is a very thick one.

Key words: three-dimensional stress field; through-the-thickness circular hole; thickness effect; stress concentration; out-of-plane constraint

CLC number: O343.4 **Document code**: A **Article ID**: 1005-1120(2014)05-0546-06

1 Introduction

It is well recognized that the stress concentration problem has been a concern for long since it is a very important phenomenon to cause premature fracture or failure of materials and structures. Consequently, knowledge of stress concentrations in the vicinity of all kinds of disfigurements, such as cracks, voids, inclusions, delaminations and porosities, is frequently required for an accurate design of structural components and much attention has been paid to the analysis of two-dimensional (2-D) and three-dimensional (3-D) stress fields in the vicinity of a circular hole/inclusion[1-8], a crack[9-15] and a notch[16-19] based on theoretical or numerical solutions. However, because of the difficulty in satisfying boundary conditions precisely, there are only a few analytical 3-D solutions available in the literatures for relatively simple configurations which have favorable conditions of symmetry.

Nearly sixty years ago, Kane, et al.[20] provided a method to obtain 3-D stress field, but still retaining the simplicity of a 2-D model. Yang, et al.[15] and Jin, et al.[10] used this assumption to analyze the effect of transverse shear on the stress field for an elastic plate with a through-thickness crack. Based on Kane and Mindlin's assumption[20], Jin, et al.[11] analyzed the interface fracture of an elastic plate bonded to a rigid substrate. Solutions of stresses and deformations were given for a semi-infinite plate perfectly bonded to a rigid substrate and subjected to uniform in-plane normal tractions at infinity. Using the same assumption, Krishnaswamy, et al.[2] investigated the stress concentration in elastic Cosserat plates with a circular hole undergoing extensional deformations. Kotousov, et

Foundation items: Supported by the National Natural Science Foundation of China (11372269,10902057).

* **Corresponding author**: Dai Longchao, Lecturer, E-mail: dai_lc@163.com.

al.[13,14,16] studied the 3-D stress distribution around a notch, circular hole and crack in an isotropic elastic plate or a transversally isotropic elastic plate based on this assumption. However, to the best knowledge of the authors, the 3-D stress solutions to a plate subjected to far field shear load have not been obtained in an explicit form yet. On the other hand, this work is valuable for analyzing the safety problem of engineering structures and systems[21-24], such as stress concentrations and fatigue behavior in air plane, ship, and so on.

The purpose of this work is to present exact 3-D solutions for the stress field in an infinite plate holding a through-the-thickness circular hole subjected to remote shear load based on Kane and Mindlin′s assumption. Based on the present theoretical solutions, the character of the in-plane stressed and stress concentration and the emphasis has been placed on the effect of the plate thickness and Poisson′s ratio on the stress behaviors.

2 Governing Equations

Consider an isotropic, elastic, infinite plate bounded by planes $z=\pm h$ with a through-the-thickness circular hole in its center, subjected to shear loading at infinite, as shown in Fig. 1. Kane and Mindlin′s kinematic assumption is adopted, namely, the displacement field in the plate has the following forms

$$u_x=u(x,y),u_y=v(x,y),u_z=\frac{z}{h}w(x,y) \quad (1)$$

Eq. (1) implies that lines being normal to the mid-plane of the plate in an un-deformed state are still normal in a deformed state and that these lines experience uniform extensional strain $w(x,y)/h$ along the z direction, where $w(x,y)$ is the out-of-plane displacement of the plate at $z=h$. With the displacement field given by Eq. (1), two out-of-plane shear stress components are linearly distributed in the thickness (z) direction.

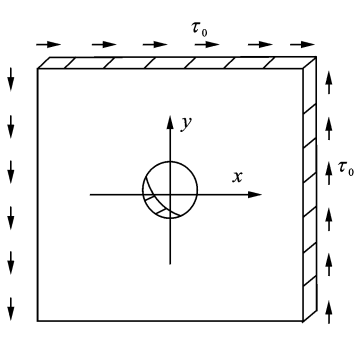

Fig. 1 Finite thickness plate with circular hole subjected to remote loadings

Following the similar procedure illustrated by Kane, et al.[20] and considering the following definitions

$$(\overline{\sigma_{\alpha\beta}},\overline{\sigma_{zz}},\overline{\kappa_{z\beta}})=\frac{1}{2h}\int_{-h}^{h}(\sigma_{\alpha\beta},\sigma_{zz},z\sigma_{z\beta})\mathrm{d}z$$
$$(\overline{\varepsilon_{\alpha\beta}},\overline{\varepsilon_{zz}},\overline{\xi_{z\beta}})=\frac{1}{2h}\int_{-h}^{h}(\varepsilon_{\alpha\beta},\varepsilon_{zz},2z\varepsilon_{z\beta})\mathrm{d}z \quad (2)$$

one obtains the following constitutive relations and equilibrium equations

$$(\overline{\varepsilon_{\alpha\beta}},\overline{\varepsilon_{zz}},\overline{\xi_{z\beta}})=\frac{1+\nu}{E}(\overline{\sigma_{\alpha\beta}},\overline{\sigma_{zz}},2\,\overline{\kappa_{z\beta}})-\frac{\nu}{E}\overline{\sigma_{kk}}(\delta_{\alpha\beta},1,0) \quad (3)$$

$$\overline{\sigma_{\alpha\beta,\beta}}=0,\quad \overline{\kappa_{z\beta,\beta}}-\overline{\sigma_{zz}}=0 \quad (4)$$

where E, ν are the Young′s modulus and the Poisson′s ratio of an isotropic material, respectively. $\overline{\sigma_{\alpha\beta}}$, $\overline{\sigma_{zz}}$, and $\overline{\varepsilon_{\alpha\beta}}$, $\overline{\varepsilon_{zz}}$ are the mean of stress components and strain components along plate thickness. $\overline{\kappa_{z\beta}}$ and $\overline{\xi_{z\beta}}$ are the components of "pinching" shear stress and strain, respectively, which play a role similar to that of the transverse shear stress and strain in the corresponding equilibrium equations of flexible plates.

In Eqs. (2−4), and throughout the remains of this paper, Greek letters indice range 1 and 2. Introduce function ϕ, similar to the Airy stress-resultant function, and φ, together with

$$\overline{\sigma_{\alpha\beta}}=\nabla^2\phi\delta_{\alpha\beta}-\phi_{\alpha\beta},\quad \overline{\kappa_{z\beta}}=\varphi_{,\beta} \quad (5)$$

Thus, the first equation of Eq. (4) is automatically satisfied, and the second equation of Eq. (4) can be simplified as

$$\overline{\sigma_{zz}}=\nabla^2\varphi \quad (6)$$

Inserting Eqs. (3, 5, 6) into the deformed harmonious equations yields

$$\nabla^4\varphi=A\nabla^2\varphi \quad (7a)$$

$$\nu\nabla^2\phi=\nabla^2\varphi-A_2\varphi \quad (7b)$$

where ∇^2 and ∇^4 are the 2-D Laplacian and biharmonic operators, respectively, and

$$A_2=\frac{6(1+\nu)}{h^2},\quad A=\frac{A_2}{1-\nu^2} \tag{8}$$

With the introduction of polar coordinates (r,θ), the formulae of stress components hold

$$\begin{aligned}&\overline{\sigma_r}=\frac{1}{r}\frac{\partial\phi}{\partial r}+\frac{1}{r^2}\frac{\partial^2\phi}{\partial^2\theta},\quad \overline{\sigma_\theta}=\frac{\partial^2\phi}{\partial^2 r}\\&\overline{\sigma_{r\theta}}=-\frac{1}{r}\frac{\partial^2\phi}{\partial r\partial\theta}+\frac{1}{r^2}\frac{\partial\phi}{\partial\theta}\\&\overline{\sigma_{zz}}=\nabla^2\varphi,\ \overline{\kappa_{zr}}=\frac{\partial\varphi}{\partial r},\ \overline{\kappa_{z\theta}}=\frac{1}{r}\frac{\partial\varphi}{\partial\theta}\end{aligned} \tag{9}$$

Consider an infinite plate containing a circular hole of radius R. The plate is loaded in far-field shear loading. In the polar coordinate systems, the boundary conditions can be expressed as follows

$$\begin{aligned}&\overline{\sigma_r}=\tau_0\sin2\theta,\quad \overline{\sigma_{r\theta}}=\tau_0\cos2\theta\quad \text{when}\quad r\to\infty\\&\overline{\sigma_r}=0,\quad \overline{\sigma_{r\theta}}=0,\quad \overline{\kappa_{zr}}=0\quad \text{when}\quad r=R\end{aligned} \tag{10}$$

3 Solution Procedure

Keeping in mind the boundary conditions Eq. (10), one seeks solutions to Eq. (7) in the form of

$$\phi(r,\theta)=\phi_2(r)\sin2\theta \tag{11a}$$

$$\varphi(r,\theta)=\varphi_2(r)\sin2\theta \tag{11b}$$

Inserting Eq. (11b) into Eq. (7a) produces

$$\varphi(r,\theta)=(c_{12}I_2(\sqrt{A}r)+c_{22}K_2(\sqrt{A}r)+c_{32}r^2+c_{42}r^{-2})\tau_0\sin2\theta \tag{12}$$

where $I_n(x)$ and $K_n(x)$ are the modified Bessel functions of order n, in which n is an integer. Since all stress components must remain bounded at infinity, Eq. (12) can be simplified as

$$\varphi(r,\theta)=(c_{22}K_2(\sqrt{A}r)+c_{32}r^2+c_{42}r^{-2})\tau_0\sin2\theta \tag{13}$$

Substituting Eq. (13) into Eq. (7) gives

$$\phi(r,\theta)=\tau_0\sin\theta\cdot\left[d_{12}r^2+d_{22}r^{-2}+\frac{A-A_2}{A\nu}c_{22}K_2(\sqrt{A}r)-\frac{A_2c_{32}}{12\nu}r^4+\frac{A_2}{4\nu}c_{42}\right] \tag{14}$$

Then, inserting Eqs. (13, 14) into Eq. (9) yields all stress components, namely

$$\frac{\overline{\sigma_r}}{\tau_0}=-\frac{\sin2\theta}{A\nu r^2}(\sqrt{A}rK_1(\sqrt{A}r)+6K_2(\sqrt{A}r))\cdot(A-A_2)c_{22}-\sin2\theta\frac{A_2c_{42}+2r^2\nu d_{12}}{\nu r^2}-\sin2\theta\frac{6d_{22}}{r^4} \tag{15a}$$

$$\frac{\overline{\sigma_\theta}}{\tau_0}=\frac{\sin2\theta}{4\nu}(K_0(\sqrt{A}r)+2K_2(\sqrt{A}r)+K_4(\sqrt{A}r))\cdot(A-A_2)c_{22}+\sin2\theta\frac{-r^2A_2c_{32}+2\nu d_{12}}{\nu}+\sin2\theta\frac{6d_{22}}{r^4} \tag{15b}$$

$$\frac{\overline{\sigma_{r\theta}}}{\tau_0}=\frac{\cos2\theta}{A\nu r^2}2(\sqrt{A}rK_1(\sqrt{A}r)+3K_2(\sqrt{A}r))\cdot(A-A_2)c_{22}+\frac{\cos2\theta}{2A\nu r^2}(AA_2(r^4c_{32}+c_{42})-4Ar^2\nu d_{12})+6d_{22}\frac{\cos2\theta}{r^4} \tag{15c}$$

$$\frac{\overline{\sigma_z}}{\tau_0}=Ac_{22}K_2(\sqrt{A}r)\sin2\theta \tag{15d}$$

$$\frac{\overline{\sigma_{zr}}}{\tau_0}=\sin2\theta\left[-\frac{\sqrt{A}c_{22}}{2}(K_1(\sqrt{A}r)+K_3(\sqrt{A}r))+2rc_{32}-\frac{2c_{42}}{r^3}\right] \tag{15e}$$

$$\frac{\overline{\sigma_{z\theta}}}{\tau_0}=\frac{2\cos2\theta}{r^3}(r^2c_{22}K_2(\sqrt{A}r)+r^4c_{32}+c_{42}) \tag{15f}$$

Note that the stress components must remain bounded at infinity. Substituting Eqs. 15(a—c, e) into the boundary conditions Eq. (10) and solving the subsequent equations for the coefficients give

$$\begin{aligned}&c_{32}=0,\quad d_{12}=-\frac{1}{2}\\&c_{22}=-\frac{8R\nu}{4\sqrt{A}K_1+RA_2(2K_0+\sqrt{A}RK_1)}\\&c_{42}=\frac{2AR^4\nu(K_1+K_3)}{4AK_1+A_2(2\sqrt{A}RK_0+AR^2K_1)}\\&d_{22}=-\frac{2R^3\left[-4A^{3/2}RK_3+A_2(\sqrt{A}R(4+AR^2)K_1+2(8+AR^2)K_2)\right]}{16A^{3/2}K_1+4AA_2R(2K_0+\sqrt{A}RK_1)}\end{aligned} \tag{16}$$

where K_n denotes $K_n(\sqrt{A}R)$, the modified Bessel functions of order n, here n is an integer.

4 Results and Discussion

It should be noted that, in this paper, the values of $\overline{\sigma_{r\theta}}/\sigma_{r\theta}$ at $r/R=1.0001$ is replaced by those at $r/R=1.0$ for analytic simplification. The effect of the plate thickness on distributions of the three normalized in-plane stresses is shown in Fig. 2. Curves of $\overline{\sigma_{r\theta}}/\sigma_{r\theta}$ are decreasing monotonously with r/R. Solutions show that for each curve of $K=\overline{\sigma_\theta}/\sigma_\theta$, there exists a minimum value,

and the position where K reaches its minimal is farther and farther away from the hole when the h/R increases. Generally speaking, the maximum deviation of the present in-plane stresses from the related plane stress solutions is at the root of the hole, and the present in-plane stress solutions agree well with the plane stress ones except for those of the locations near the hole.

The effect of Poisson's ratio on distributions of the three normalized in-plane stresses is shown in Fig. 3. It can be found that the bigger the value of Poisson's ratio, the heavier the maximum deviation of the present solutions from the related plane stress solutions. From Figs. 2, 3, it can be found that the influence of Poisson's ratio on the distributions of the in-plane stress is stronger than that of the plate thickness. Furthermore, only the in-plane stresses near the hole depend on plate thickness and Poisson's ratio. Outside this region, the effect of plate thickness and Poisson's ratio on the distributions of in-plane stresses can be neglected. Some numerical results are obtained based on finite element (FE) analysis software Abaqus for the value of K on the section at $\theta=3\pi/4$ in Fig. 2(b). It can be found that although there are differences between the present solutions and FE results, these differences are negligible in terms of numerical value in fact. Thus the present solutions are consistent with those using finite element methods (FEM) from a numerical standpoint.

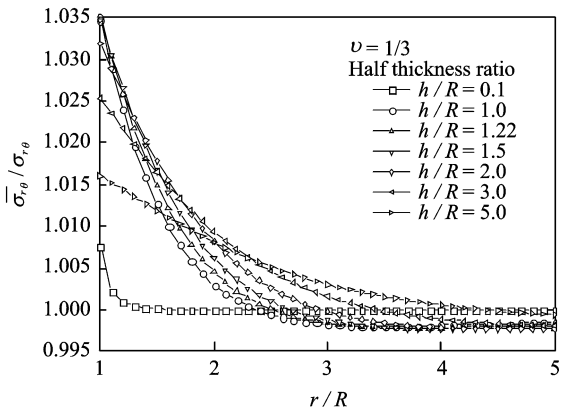

(a) $\overline{\sigma_{r\theta}}/\sigma_{r\theta}$ on section at $\theta=\pi/2$

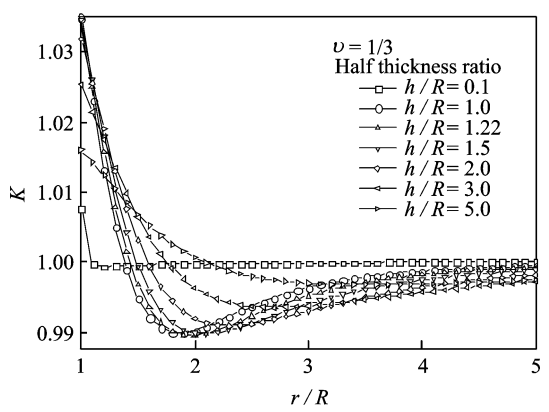

(b) $K=\overline{\sigma_\theta}/\sigma_\theta$ on section at $\theta=3\pi/4$

Fig. 2 Distributions of three in-plane stress ratios with r/R for different h/R with the Poisson's ratio $\nu=1/3$

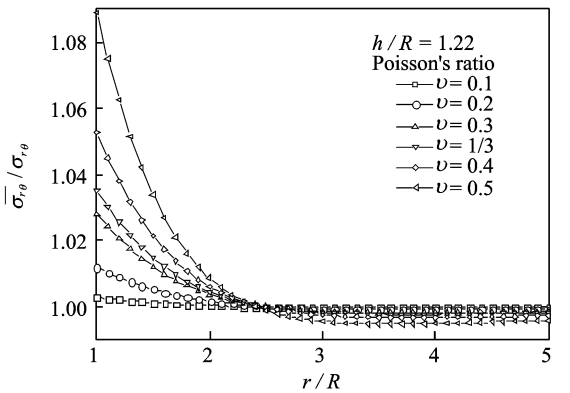

(a) $\overline{\sigma_{r\theta}}/\sigma_{r\theta}$ on section at $\theta=\pi/2$

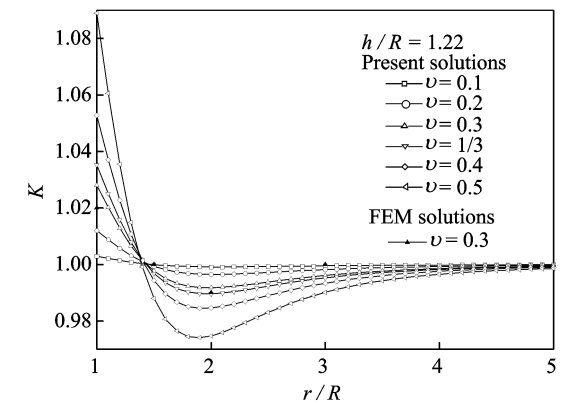

(b) $K=\overline{\sigma_\theta}/\sigma_\theta$ on section at $\theta=3\pi/4$

Fig. 3 Distributions of three in-plane stress ratios with r/R for different ν with $h/R=1.22$

Fig. 4 shows the variations of the stress concentration K_t at the root of the hole with the semi-thickness ratio h/R and $\theta=3\pi/4$ for different Poisson's ratio ν. It is seen that K_t increases with the increase of ν. K_t rises rapidly when the plate is thin and reaches its peak values 4.011 77 at $\nu=0.1$ and $h/R\doteq1.1$; 4.048 06 at $\nu=0.2$ and

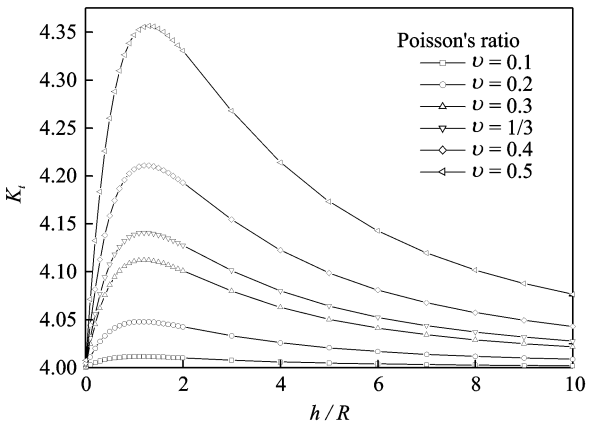

Fig. 4 Variations of stress concentration factor K_t at root of circular hole with semi-thickness ratio h/R for different Poisson's ratio ν with $\theta=3\pi/4$

$h/R\doteq 1.2$; 4.112 31 at $\nu=0.3$ and $h/R\doteq 1.2$; 4.140 92 at $\nu=1/3$ and $h/R\doteq 1.2$; 4.210 94 at $\nu=0.4$ and $h/R\doteq 1.3$; and 4.356 51 at $\nu=0.5$ and $h/R\doteq 1.3$, respectively. Outside this region, K_t decreases with the increase of h/R and approaches its limit value 4.0. It is clearly seen that the increase of the stress concentration factor for an infinite plate with a through-the-thickness hole subjected to shear loading can reach up to 8.9% approximately.

Variations of the out-of-plane stress constraint factor $T_z=\dfrac{\overline{\sigma_{zz}}}{\nu(\overline{\sigma_r}+\overline{\sigma_\theta})}$ at the root of circular hole with semi-thickness ratio h/R for different Poisson's ratio ν are plotted in Fig. 5. It shows

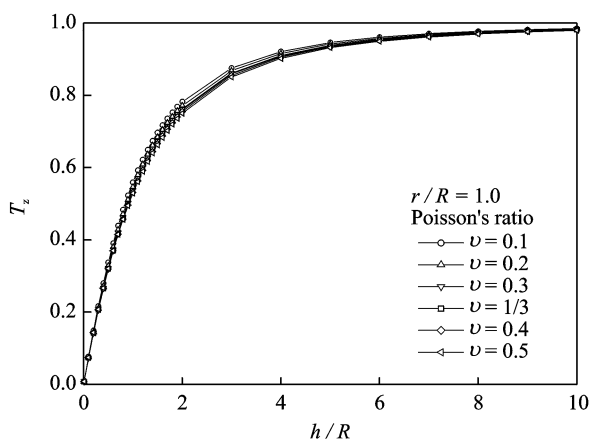

Fig. 5 Variations of out-of-plane stress constraint factor T_z at root of circular hole with semi-thickness ratio h/R for different Poisson's ratio ν with $\theta=3\pi/4$.

that the out-of-plane stress constraint factor T_z can reach 0.985 at $h/R=10$, and that the out-of-plane constraint is nearly independent of the Poisson's ratio on the section at $\theta=3\pi/4$. Furthermore, based on the present solutions of all stress components, Eq. (15), it can be found that the variations of the out-of-plane stress constraint factor T_z are independent of the section of θ at the root of circular hole.

5 Conclusions

By using Kane and Mindlin's assumption and the stress function method, theoretical solutions to the 3-D stress field are obtained for an isotropic infinite plate of arbitrary thickness holding a through-the-thickness circular hole subjected to remote shear load. Based on the present solutions, an analysis is performed on the characteristics of 3-D stress field and the emphasis has been placed on the effects of plate thickness and Poisson's ratio on the stress behaviors. It is found that the influence of Poisson's ratio on the deviation of the present in-plane stresses from the related plane stress solutions is stronger than that of plate thickness, and that only near the hole the deviation of the present in-plane stresses depends on plate thickness and Poisson's ratio for the case of far field shear loadings. When the plate is thin, the stress concentration factor rises rapidly and reaches its peak value. Then it decreases with the increase of plate thickness and approaches its limit value 4.0. It can be found that the increase of the stress concentration factor for an infinite plate with a through-the-thickness hole subjected to shear loading can reach 8.9% approximately. Moreover, the out-of-plane stress constraint factor T_z can reach 0.985 at $h/R=10$, and the out-of-plane constraint is nearly independent of the Poisson's ratio.

References:

[1] Folias E S, Wang J J. On the three-dimensional stress field around a circular hole in a plate of arbitrary thickness [J]. Computational Mechanics, 1990, 6(5/6): 379-391.

[2] Krishnaswamy S, Jin Z H, Batra R C. Stress concentration in an elastic Cosserat plate undergoing extensional deformations [J]. ASME Journal of Applied Mechanics, 1998, 65(1): 66-70.

[3] Kotousov A, Wang C H. Three-dimensional solutions for transversally isotropic plates [J]. Composite Structures, 2002, 57(1/2/3/4): 445-452.

[4] Chaudhuri R A. Three-dimensional asymptotic stress field in the vicinity of the circumferential line of intersection of an inclusion and plate surface [J]. International Journal of Fracture, 2003, 119(3): 195-222.

[5] Chaudhuri R A. Three-dimensional asymptotic stress field in the vicinity of the line of intersection of a circular cylindrical through/part-through open/rigidly plugged hole and a plate[J]. International Journal of Fracture, 2003, 122(1/2): 65-88.

[6] Penado F E, Folias E S. The three-dimensional stress field around a cylindrical inclusion in a plate of arbitrary thickness [J]. International Journal of Fracture, 1989, 39(1/2): 129-146.

[7] Yang Z, Kim C B, Cho C, et al. The concentration of stress and strain in finite thickness elastic plate containing a circular hole [J]. International Journal of Solids and Structures, 2008, 45(3/4): 713-731.

[8] Dai L C, Wang X, Liu F. Stress concentrations around a circular hole in an infinite plate of arbitrary thickness [J]. Structure Engineering Mechanics, 2010, 34(2): 143-157.

[9] Folias E S. On the three-dimensional theory of cracked plates [J]. ASME Journal of Applied Mechanics, 1975, 42(3): 663-674.

[10] Jin Z H, Hwang K C. An analysis of three-dimensional effects near the tip of a crack in an elastic plate [J]. Acta Mechanica Solida Sinica, 1989, 2(4): 387-401.

[11] Jin Z H, Batra R C. A crack at the interface between a Kane-Mindlin plate and a rigid substrate [J]. Engineering Fracture Mechanics, 1997, 57(4): 343-354.

[12] Jin Z H, Batra R C. Dynamic fracture of a Kane-Mindlin plate [J]. Theoretical and Applied Fracture Mechanics, 1997, 26(3): 199-209.

[13] Kotousov A, Tan P J. Effect of the plate thickness on the out-of-plane displacement field of a cracked elastic plate loaded in mode I [J]. International Journal of Fracture, 2004, 127(1): L97-L103.

[14] Kotousov A, Wang C H. Fundamental solutions for the generalized plane strain theory [J]. International Journal of Engineering Science, 2002, 40(15): 1775-1790.

[15] Yang W, Freund L B. Transverse shear effects for through-crack in an elastic plate [J]. International Journal of Solids and Structures, 1985, 21: 977-994.

[16] Kotousov A, Wang C H. Three-dimensional stress constraint in an elastic plate with a notch [J]. International Journal of Solids and Structures, 2002, 39(16): 4311-4326.

[17] Lazzarin P, Tovo R. A unified approach to the evaluation of linear elastic stress fields in the neighborhood of cracks and notches [J]. International Journal of Fracture, 1996, 78(1): 3-19.

[18] Filippi S, Lazzarin P, Tovo R. Developments of some explicit formulas useful to describe elastic stress fields ahead of notches in plates [J]. International Journal of Solids and Structures, 2002, 39(17): 4543-4565.

[19] Filippo B, Lazzarin P, Wang C H. Three-dimensional linear elastic distributions of stress and strain energy density ahead of V-shaped notches in plates of arbitrary thickness [J]. International Journal of Fracture, 2004, 127(3): 265-281.

[20] Kane T R, Mindlin R D. High-frequency extensional vibrations of plates [J]. ASME Journal of Applied Mechanics, 1956, 23(3): 277-283.

[21] Meng B, She C. Finite element analyses of stress intensity factors of cracks at V-notches [J]. Journal of Nanjing University of Aeronautics and Astronautics, 2009,41(1):126-129. (in Chinese)

[22] Xue H, Wu T, Bathias C. Gigacycle fatigue behavior of cast aluminum in tension and torsion loading [J]. Transactions of Nanjing University of Aeronautics and Astronautics, 2011,28(1):2-37.

[23] Sun W, Guo L, Tong M, et al. Post bucking analysis and structure optimization of integral fuselage panel subjected to axial compression load [J]. Transactions of Nanjing University of Aeronautics and Astronautics, 2010, 27(4): 281-287.

[24] Chen B, Zeng, J, Jia J, et al. DFR method based on finite element analysis [J]. Journal of Nanjing University of Aeronautics and Astronautics, 2012, 44(6):888-892. (in Chinese)

(Executive editor: Zhang Tong)